Thermodynamics of a one-dimensional frustrated spin-$\frac{1}{2}$ Heisenberg ferromagnet

M. Härtel and J. Richter
Institut für Theoretische Physik, Otto-von-Guericke-Universität Magdeburg, D-39016 Magdeburg, Germany

D. Ihle
Institut für Theoretische Physik, Universität Leipzig, D-04109 Leipzig, Germany

S.-L. Drechsler
Leibniz-Institut für Festkörper- und Werkstoffforschung Dresden, D-01171 Dresden, Germany
(Received 9 July 2008; revised manuscript received 2 October 2008; published 12 November 2008)

We calculate the thermodynamic quantities (correlation functions $\langle \mathbf{S}_0 \mathbf{S}_n \rangle$, correlation length ξ, spin susceptibility χ, and specific heat C_V) of the frustrated one-dimensional spin-half J_1-J_2 Heisenberg ferromagnet, i.e., for $J_2 < 0.25|J_1|$, using a rotation-invariant Green's-function formalism and full diagonalization of finite lattices. We find that the critical indices are not changed by J_2, i.e., $\chi = y_0 T^{-2}$ and $\xi = x_0 T^{-1}$ at $T \to 0$. However, the coefficients y_0 and x_0 linearly decrease with increasing J_2 according to the relations $y_0 = (1-4J_2/|J_1|)/24$ and $x_0 = (1-4J_2/|J_1|)/4$, i.e., both coefficients vanish at $J_2 = 0.25|J_1|$ indicating the zero-temperature phase transition that is accompanied by a change in the low-temperature behavior of χ (ξ) from $\chi \propto T^{-2}$ ($\xi \propto T^{-1}$) at $J_2 < 0.25|J_1|$ to $\chi \propto T^{-3/2}$ ($\xi \propto T^{-1/2}$) at $J_2 = 0.25|J_1|$. In addition, we detect the existence of an additional low-temperature maximum in the specific heat when approaching the critical point at $J_2 = 0.25|J_1|$.

DOI: 10.1103/PhysRevB.78.174412 PACS number(s): 75.10.Jm, 75.40.Cx, 75.40.Gb

I. INTRODUCTION

Low-dimensional quantum magnets represent an ideal playground to study systems with strong quantum and thermal fluctuations.[1] In particular, much attention has been paid to the one-dimensional (1D) J_1-J_2 quantum Heisenberg model, which may serve as a canonical model to study frustration effects in low-dimensional quantum magnets. Although this model has been studied frequently (see Ref. 2, and references therein), the model deserves further attention to detect unknown features of this quantum many-body system especially in the case of ferromagnetic nearest-neighbor (NN) interaction $J_1 < 0$.[3–11] From the experimental side, recent studies have demonstrated that edge-shared chain cuprates represent a family of quantum magnets for which the 1D J_1-J_2 Heisenberg model is an appropriate starting point for a theoretical description. Among others, we mention $LiVCuO_4$, $LiCu_2O_2$, $NaCu_2O_2$, Li_2ZrCuO_4, and Li_2CuO_2,[12–21] which were identified as quasi-1D frustrated spin-1/2 magnets with a ferromagnetic NN in-chain coupling $J_1 < 0$ and an antiferromagnetic next-nearest-neighbor (NNN) in-chain coupling $J_2 > 0$. The Hamiltonian of their 1D subsystems considered in this paper is then given by

$$H = J_1 \sum_{\langle i,j \rangle} \mathbf{S}_i \mathbf{S}_j + J_2 \sum_{[i,j]} \mathbf{S}_i \mathbf{S}_j, \tag{1}$$

where $\langle i,j \rangle$ runs over the NN and $[i,j]$ over the NNN bonds. For the model (1) the ferromagnetic ground state (GS) gives way for a singlet GS with spiral correlations at the critical point $J_2 = 0.25|J_1|$.[7,22]

The edge-shared chain cuprates have attracted much attention due to the observation of incommensurate spiral spin ordering at low temperature. Hence, in these compounds the antiferromagnetic NNN exchange J_2 is strong enough to destroy the ferromagnetic GS favored by the ferromagnetic J_1. On the other hand, several materials that considered as model systems for 1D spin-1/2 ferromagnets, such as Tetramethylammonium Copper Chloride (TMCuC$[(CH_3)_4NCuCl_3]$) (Ref. 23) and *p*-nitrophenyl nitronyl nitroxide (*p*-NPNN) ($C_{13}H_{16}N_3O_4$),[24] might have also a weak frustrating NNN exchange interaction $J_2 < -0.25J_1$. Moreover, recent investigations suggest that Li_2CuO_2 is a quasi-1D spin-1/2 system with a dominant ferromagnetic J_1 and weak frustrating antiferromagnetic $J_2 \approx 0.2|J_1|$.[21]

Although for $J_2 < -0.25J_1$ the GS remains ferromagnetic, the frustrating J_2 may influence the thermodynamics substantially, in particular, near the zero-temperature critical point at $J_2 = 0.25|J_1|$. The investigation of this issue is the aim of this paper. The study of the 1D J_1-J_2 Heisenberg model is faced with the problem that, due to the J_2 term, neither the Bethe-ansatz solution nor the quantum Monte Carlo method is applicable. Hence, we use (i) the full exact diagonalization (ED) of finite systems of up to $N=22$ lattice sites and (ii) the second-order Green's-function technique[25] that has been applied recently successfully to low-dimensional quantum spin systems.[26–29] For example, in Ref. 27, by comparison with Bethe-ansatz data it has been demonstrated that this method leads to qualitatively correct results for the thermodynamics of the 1D Heisenberg ferromagnet in a magnetic field. As the most prominent feature, a field-induced extra low-temperature maximum in the specific heat has been found[27] and characterized as a peculiar quantum effect.[27,29]

II. FULL DIAGONALIZATION OF FINITE LATTICES

Using Schulenburg's SPINPACK (Ref. 30) and exploiting the lattice symmetries and the fact that $S^z = \sum_i S_i^z$ commutes with H, we are able to calculate the exact thermodynamics for periodic chains of up to $N=22$ spins. The comparison of results for $N=12$, 14, 16, 18, 20, and 22 allows to estimate the finite-size effects. The largest matrix which has to be diagonalized for $N=22$ has $29\,414 \times 29\,414$ matrix elements.

III. SPIN-ROTATION-INVARIANT GREEN'S-FUNCTION THEORY

To calculate the spin-correlation functions and the thermodynamic quantities, we determine the transverse spin susceptibility $\chi_q^{+-}(\omega)=-\langle\langle S_q^+;S_{-q}^-\rangle\rangle_\omega$ (here, $\langle\langle\ldots;\ldots\rangle\rangle_\omega$ denotes the two-time commutator Green's function[31]) by the spin-rotation-invariant Green's-function method (RGM).[25,26] Using the equations of motion up to the second step and supposing rotational symmetry, i.e., $\langle S_i^z\rangle=0$, we obtain $\omega^2\langle\langle S_q^+;S_{-q}^-\rangle\rangle_\omega=M_q+\langle\langle-\ddot{S}_q^+;S_{-q}^-\rangle\rangle_\omega$ with $M_q=\langle[[S_q^+,H],S_{-q}^-]\rangle$ and $-\ddot{S}_q^+=[[S_q^+,H],H]$. For the model (1) the moment M_q is given by the exact expression

$$M_q = -4\sum_{n=1,2} J_n C_n(1-\cos nq), \tag{2}$$

where $C_n=\langle S_0^+S_n^-\rangle=2\langle S_0^zS_n^z\rangle$. The second derivative $-\ddot{S}_q^+$ is approximated as indicated in Refs. 25–29. That is, in $-\ddot{S}_i^+$ we adopt the decoupling $S_i^+S_j^+S_k^-=\alpha\langle S_j^+S_k^-\rangle S_i^+ + \alpha\langle S_i^+S_k^-\rangle S_j^+$, where in the case $J_2<-0.25J_1$ with a ferromagnetic GS the vertex parameter α can be assumed in a good approximation to be independent of the range of the associated spin correlators (see the discussion below). We obtain $-\ddot{S}_q^+=\omega_q^2 S_q^+$ and

$$\chi_q^{+-}(\omega) = -\langle\langle S_q^+;S_{-q}^-\rangle\rangle_\omega = \frac{M_q}{\omega_q^2-\omega^2}, \tag{3}$$

with

$$\omega_q^2 = \sum_{n,m(=1,2)} J_nJ_m(1-\cos nq)[K_{n,m}+4\alpha C_n(1-\cos mq)], \tag{4}$$

where $K_{n,n}=1+2\alpha(C_{2n}-3C_n)$, $K_{1,2}=2\alpha(C_3-C_1)$, and $K_{2,1}=K_{1,2}+4\alpha(C_1-C_2)$. From the Green's function (3) the correlation functions $C_n=\frac{1}{N}\Sigma_q C_q e^{iqn}$ of arbitrary range n are determined by the spectral theorem[31]

$$C_q = \langle S_q^+S_{-q}^-\rangle = \frac{M_q}{2\omega_q}[1+2n(\omega_q)], \tag{5}$$

where $n(\omega_q)=(e^{\omega_q/T}-1)^{-1}$ is the Bose function. By the operator identity $S_i^+S_i^-=\frac{1}{2}+S_i^z$ we get the sum rule $C_0=\frac{1}{N}\Sigma_q C_q=\frac{1}{2}$. The uniform static spin susceptibility $\chi=\lim_{q\to 0}\chi_q$, where $\chi_q=\chi_q(\omega=0)$ and $\chi_q(\omega)=\frac{1}{2}\chi_q^{+-}(\omega)$, is given by

$$\chi = -\frac{2}{\Delta}\sum_{n=1,2} n^2 J_n C_n, \quad \Delta = \sum_{n,m(=1,2)} n^2 J_n J_m K_{n,m}. \tag{6}$$

The correlation length ξ may be calculated from the expansion of the static spin susceptibility around $q=0$ (see, e.g., Refs. 25 and 29) $\chi_q=\chi/(1+\xi^2q^2)$. The ferromagnetic long-range order, occurring in the 1D model at $T=0$ only, is described by the condensation term C (Ref. 25) according to $C_n(0)=\frac{1}{N}\Sigma_{q(\neq 0)}(M_q/2\omega_q)e^{iqn}+C$. Equating this expression for $n\neq 0$ to the exact result $C_{n\neq 0}(0)=\frac{1}{6}$ $[\langle\vec{S}_0\vec{S}_{n\neq 0}\rangle(0)=\frac{1}{4}]$, the ratio $M_q/2\omega_q$ must be independent of q because $C_{n\neq 0}$ is independent of n. This requires the equations $K_{n,m}(0)=0$ [cf. Eqs. (2) and (4)], which yield $\alpha(0)=\frac{3}{2}$. Then, we get $\omega_q(0)=\frac{3}{2}M_q(0)$ and $C=\frac{1}{6}$, where the sum rule $C_0=\frac{1}{2}$ is fulfilled. In Eq. (6), we have $\Delta(0)=0$, so that χ diverges as $T\to 0$ indicating the ferromagnetic phase transition.

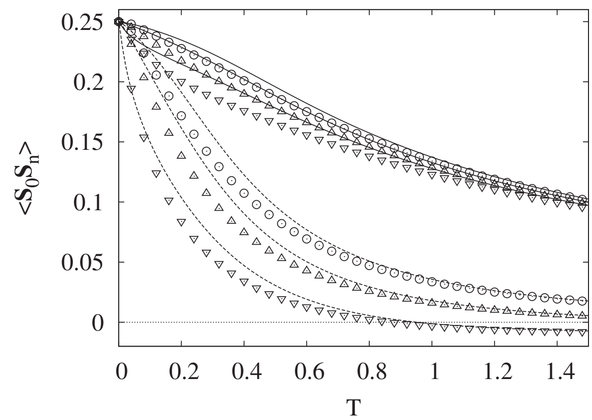

FIG. 1. NN (solid) and NNN (dashed) spin-correlation function for $J_2=0$, 0.1, and 0.2, from top to bottom, calculated by RGM (lines) and ED (open symbols; $N=20$).

Let us discuss the used assumption that the vertex parameter α is independent of the distance l. For that, we consider an extended decoupling with four different parameters α_l ($l=1,\ldots,4$) attached to the four correlators C_l appearing in ω_q^2 [cf. Eq. (4)]. At $T=0$, the four equations $K_{n,m}=0$ ($n,m=1,2$) yield the solutions $\alpha_l(0)=\frac{3}{2}$. On the other hand, in the high-temperature limit all vertex parameters approach unity.[25] Because we have identical vertex parameters at $T=0$ and for $T\to\infty$, we put $\alpha_l=\alpha$ in the whole temperature region, as was done above.

To evaluate the thermodynamic properties, the correlators C_l ($l=1,\ldots,4$) and the vertex parameter α have to be determined as numerical solutions of a coupled system of five nonlinear algebraic self-consistency equations for C_l including the sum rule $C_0=\frac{1}{2}$ according to Eq. (5). Tracing the RGM solution to very low temperature, we find that it becomes less trustworthy for J_2 approaching $J_2=0.25|J_1|$. Therefore, below we will present RGM results for $J_2\leq 0.2|J_1|$ only.

IV. RESULTS

Hereafter, we put $|J_1|=1$. First we consider the NN and NNN correlation functions shown in Fig. 1. The RGM results agree qualitatively well with the ED data. Note that the difference between ED and RGM results at low temperature might be partially attributed to finite-size effects in the ED data. For larger temperature $T\gtrsim 1$, the agreement becomes perfect. With increasing frustration the correlation functions decrease, where the NNN and further-distant correlators decay much stronger than the NN correlator (interestingly, for $J_2=0.2$ the NNN correlator changes the sign at $T\approx 1$). This frustration effect is reflected in the correlation length ξ depicted in the inset of Fig. 2. At $T=0$, ξ and the uniform static

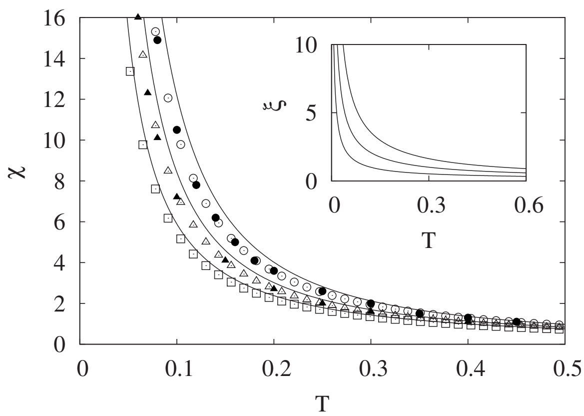

FIG. 2. Uniform static spin susceptibility calculated by RGM (solid lines) and ED (open symbols; N=20) for J_2=0, 0.125, and 0.2, from right to left, and by TMRG (filled symbols) for J_2=0 and 0.125 (Ref. 6). The inset shows the correlation length obtained by RGM for J_2=0, 0.125, and 0.2, from right to left.

spin susceptibility χ diverge due to the ferromagnetic GS. With growing temperature, the decay of ξ increases with increasing J_2. As shown in Fig. 2, our ED data for χ are in excellent agreement with the results of the transfer-matrix renormalization-group (TMRG) study of Ref. 6 and agree well with the RGM results. The susceptibility decreases with increasing J_2 because this antiferromagnetic interaction counteracts the spin orientation along a uniform magnetic field.

Next, we investigate the critical behavior of χ and ξ for $T\to 0$ in more detail. To study the influence of the frustration on the critical behavior we follow Refs. 32 and 33. The critical indices γ for χ and ν for ξ can be obtained by analyzing the RGM data for $-\frac{d\log(\chi)}{d\log(T)}$ and $-\frac{d\log(\xi)}{d\log(T)}$ for $T\to 0$. We find that $\gamma=2$ and $\nu=1$ are independent of J_2 for $J_2<0.25$. Going beyond the leading order in T, we know from Bethe-ansatz data[32,33] and from the renormalization-group technique[34] that the low-temperature behavior of the susceptibility and the correlation length of the unfrustrated 1D spin-1/2 Heisenberg ferromagnet is given by

$$\chi T^2 = y_0 + y_1\sqrt{T} + y_2 T + \mathcal{O}(T^{3/2}) \tag{7}$$

and

$$\xi T = x_0 + x_1\sqrt{T} + x_2 T + \mathcal{O}(T^{3/2}). \tag{8}$$

Here we adopt this expansion suggested by the existence of the ferromagnetic critical point at $T=0$ but with J_2-dependent coefficients for the frustrated model (1). To determine the coefficients y_0 and x_0, in Figs. 3 and 4 we show the quantities χT^2 and ξT versus $\sqrt{T}$. Again we find a good agreement of the ED for χT^2 with Bethe-ansatz and TMRG data down to quite low temperature. The RGM results for χT^2 and ξT deviate slightly from the Bethe-ansatz and TMRG data for finite temperature. The behavior of the leading coefficients y_0 and x_0 and the next-order coefficients y_1 and x_1 can be extracted from the data for χT^2 and ξT by fitting these data to Eqs. (7) and (8). For the RGM we use data points up to a cutoff temperature $T=T_{\text{cut}}$. Although we find that the data fit

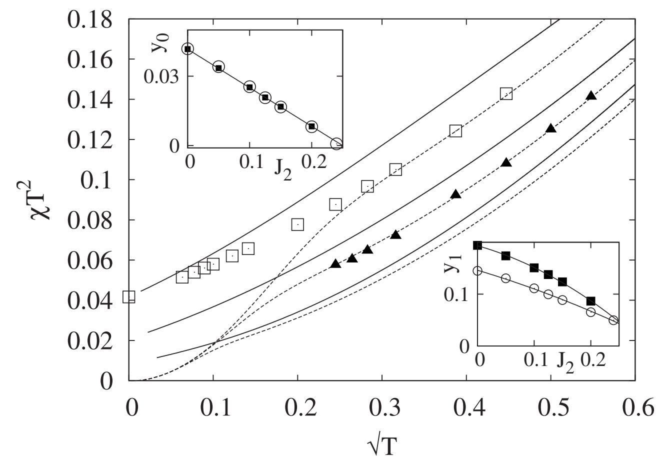

FIG. 3. χT^2 versus $\sqrt{T}$ calculated by RGM (solid lines) and ED (N=20; dashed lines) for J_2=0, 0.125, and 0.2, from top to bottom. For comparison we present also Bethe-ansatz data (open squares) for J_2=0 (Ref. 32) and TMRG data (filled triangles) for J_2=0.125 (Ref. 6). The upper inset shows the coefficient $y_0=\lim_{T\to 0}\chi T^2$ obtained by the RGM (filled squares) and ED (open circles) in dependence on J_2 as well as a linear fit of the RGM data points (solid line). The lower inset shows the coefficient y_1 [cf. Eq. (7)] obtained by the RGM (filled squares) and ED (open circles) in dependence on J_2 as well as a quadratic fit of the data points (solid line).

is almost independent of the value of T_{cut}, we choose T_{cut} =0.005, which gives optimal coincidence with Bethe-ansatz results available for J_2=0 (see below). On the other hand, the ED data at very low temperature are affected by finite-size effects. To circumvent this problem, we proceed as follows. We first determine the temperature T_{ED} down to which the first four digits of the specific heat per site $C_V(T)$ for N=20 and 22 coincide. (We use the specific heat to determine T_{ED} because $C_V(T)$ is most sensitive to finite-size effects at low

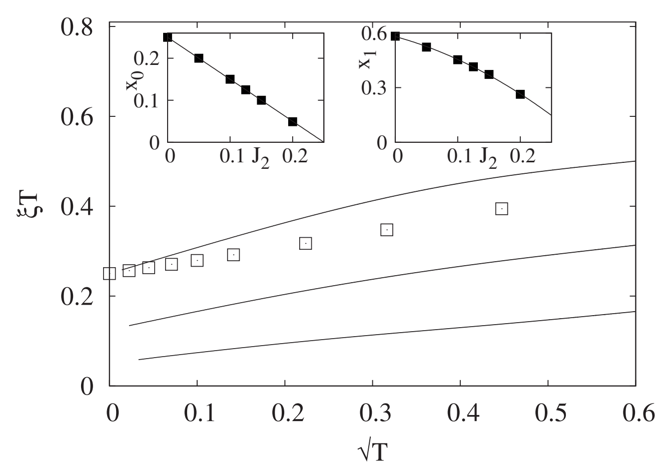

FIG. 4. ξT versus $\sqrt{T}$ by the RGM (solid lines) for J_2=0, 0.125, and 0.2, from top to bottom. For comparison we present also Bethe-ansatz data (open squares) for J_2=0 (Ref. 33). The left inset shows the coefficient $x_0=\lim_{T\to 0}\xi T$ obtained by the RGM (filled squares) in dependence on J_2 as well as a linear fit of the RGM data points (solid line). The right inset shows the coefficient x_1 [cf. Eq. (8)] obtained by the RGM (filled squares) in dependence on J_2 as well as a quadratic fit of the data points (solid line).

temperature; see also below.) Then we use the ED data points for χT^2 in the temperature region $T_{ED} \leq T \leq T_{ED} + T_{cut}$ to fit them to Eq. (7). We find that T_{ED} varies from 0.22 at $J_2=0$ to 0.03 at $J_2=0.24$. Obviously, we have to use ED data points at higher temperature for the fit in comparison to the RGM fit, in particular, at small values for J_2. The results for y_0 and y_1 as well as for x_0 and x_1 are shown in the insets of Figs. 3 and 4. It is obvious that the values for y_0 determined by RGM and ED are very close to each other. Note that for the unfrustrated 1D ferromagnet the quantities y_0 and x_0 were calculated by the RGM previously in Ref. 35. It was found that $y_0=1/24 \approx 0.041\,667$ and $x_0=1/4$, which agrees with the Bethe-ansatz results of Refs. 32 and 33 [note that χ defined in Ref. 32 is larger by a factor of 4 than χ given by Eq. (6)]. Our RGM data confirm these findings (see also Ref. 29). The fitting of the ED data at $J_2=0$ yields $y_0=0.0418$, which is still in reasonable agreement with the Bethe-ansatz result. Including frustration $J_2>0$, we find an almost linear decrease in y_0 as well in x_0 with J_2 down to zero at $J_2=0.25$ (cf. the insets of Figs. 3 and 4). A linear fit of the RGM data points yields the relations

$$y_0 = (1-4J_2)/24, \quad x_0 = (1-4J_2)/4, \tag{9}$$

which describe the RGM data in high precision. The vanishing of y_0 and of x_0 at $J_2=0.25$ reflects the zero-temperature phase transition at this point and indicates the change in the low-temperature behavior of the physical quantities at the critical point. Using the same J_2 data points as in the insets of Figs. 3 and 4, a polynomial fit according to $y_1=a_y+b_yJ_2+c_yJ_2^2$ ($x_1=a_x+b_xJ_2+c_xJ_2^2$), indeed, yields, at $J_2=0.25$, finite values $y_1=0.047$ for RGM and $y_1=0.043$ for ED and $x_1=0.147$ (RGM only). Hence, our data suggest a change in the low-temperature behavior of χ (ξ) from $\chi \propto T^{-2}$ ($\xi \propto T^{-1}$) at $J_2<0.25$ to $\chi \propto T^{-3/2}$ ($\xi \propto T^{-1/2}$) at the zero-temperature critical point $J_2=0.25$. Let us mention here again that our results for the critical indices γ and ν at $J_2=0.25$ are based on the validity of Eqs. (7) and (8) and the extrapolation of our data from $J_2<0.25$ to $J_2=0.25$. A slightly different index γ also being below the "ferromagnetic" value $\gamma_F=2$ discussed above, namely, $\gamma=4/3$, is obtained[36] if one employs the modified spin-wave theory by Takahashi[37] at $J_2=0.25$.

The next quantity we consider is the specific heat C_V. In Fig. 5 our RGM and ED results for C_V are compared with the TMRG data.[6] Obviously, the ED results are in a very good agreement with the TMRG data. The deviation at low temperature, appearing for $J_2=0.125$ as an increased value of C_V for $0.02 \lesssim T \lesssim 0.1$, is ascribed to finite-size effects (see also the discussion below). For larger values of J_2 the specific heat shows another interesting low-temperature feature (see Fig. 6). In the region $0.125<J_2<0.25$ with a ferromagnetic GS, the specific heat exhibits two maxima. Besides the broad maximum at $T\approx 0.6$, an additional frustration-induced low-temperature maximum appears, which is found by the ED and RGM methods for $J_2 \gtrsim 0.125$ and $\gtrsim 0.16$, respectively. As shown by a detailed analysis (see also below), the behavior of C_V at very low temperature is appreciably affected by finite-size effects. In particular, in the ED data, the low-temperature maximum is superimposed by a quite sharp extra finite-size peak, as can be clearly seen in Fig. 6 for $J_2=0.24$. In view of this, the height and the position of the true additional low-temperature maximum cannot be extracted unambiguously from the ED data; however, its existence is not questioned by this ambiguity. On the other hand, the RGM (see inset of Fig. 6) yields a shift of the maximum to lower temperature with increasing frustration.

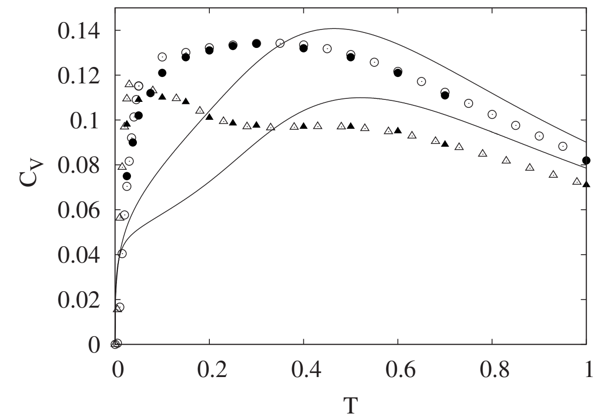

FIG. 5. Specific heat obtained by RGM (solid lines), ED (open symbols; $N=20$), and TMRG (filled symbols; Ref. 6) for $J_2=0$ and 0.125, from top to bottom.

To illustrate the finite-size effects at low temperature, in Fig. 7 the ED data for the specific heat for $J_2=0.2$ and 0.24 and different chain lengths are plotted. As already discussed above, the first four digits of the $C_V(T)$ data for $N=20$ and 22 coincide down to $T_{ED}\approx 0.04$ ($T_{ED}\approx 0.03$) for $J_2=0.2$ ($J_2=0.24$). (Note again that for $J_2=0$ the corresponding value $T_{ED}\approx 0.22$ is much larger.) Below T_{ED} finite-size effects become relevant (cf. Fig. 7). However, from Fig. 7 it is also evident that the extra low-temperature finite-size peak behaves monotonously with N. Hence, a finite-size extrapolation of the height c_{peak} and the position T_{peak} of the extra peak is reasonable. We have tested several extrapolation schemes and found that a three-parameter fit based on the formula $a(N)=a_0+a_1/N^2+a_2/N^4$ is well appropriate to extrapolate both c_{peak} and T_{peak} to $N\to\infty$. The results of such an extrapolation are shown as filled squares in Fig. 7. The ex-

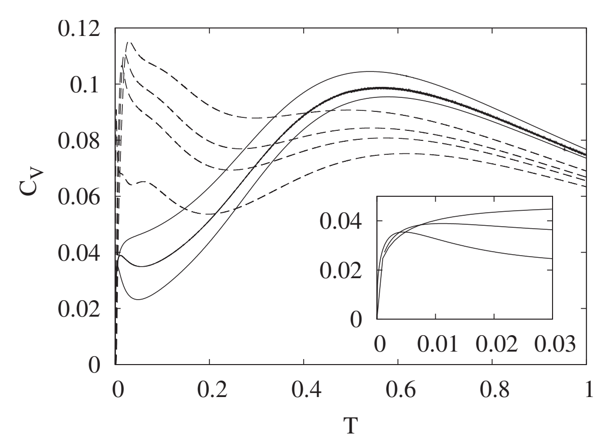

FIG. 6. Specific heat calculated by RGM (solid) and ED (dashed curve; $N=20$) for $J_2=0.15$, 0.18, 0.2, and 0.24, from top to bottom. The inset exhibits the RGM results in an enlarged scale. Note that for $J_2=0.24$ only ED data are shown.

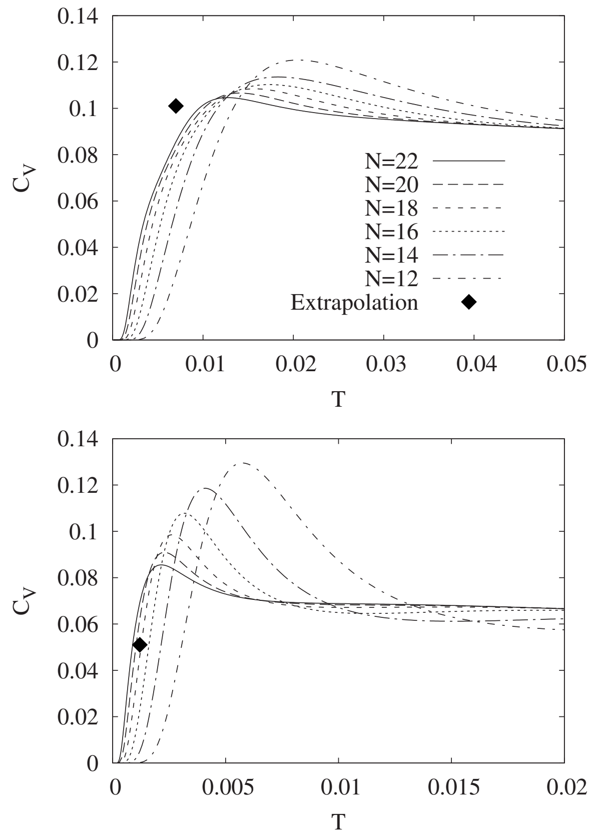

FIG. 7. Finite-size dependence of the low-temperature specific heat for $J_2=0.2$ (upper panel) and 0.24 (lower panel). The lines represent ED data for $N=12$, 14, 16, 18, 20, and 22, from top to bottom.

trapolated data points indicate that the extra peak indeed is a finite-size effect and it vanishes for $N\to\infty$. However, it is also obvious that the characteristic steep decay of the specific heat down to $T=0$ starts at lower temperature T^* when approaching the zero-temperature critical point (we find $T^* \approx 0.05$, 0.0007, and 0.002 for $J_2=0$, 0.2, and 0.24, respectively). This behavior is in accordance with the shift of the low-temperature RGM maximum in C_V mentioned above and is relevant for low-temperature experiments on quasi-1D ferromagnets.

Finally, let us mention that in an early paper by Tonegawa and Harada[3] and also recently by Heidrich-Meisner *et al.*[5] and Lu *et al.*[6] a double-maximum structure in C_V was already found for $0.25 \leq J_2 \lesssim 0.4$, however, with a low-temperature maximum that becomes much more pronounced approaching the critical point. In this case, the low-temperature peak in $C_V(T)$ was ascribed to excitations from a singlet GS to a low-lying ferromagnetic multiplet.[5] In our case $J_2 < 0.25$. Above the fully polarized ferromagnetic GS multiplet many low-lying multiplets exist, and the appearance of the additional low-temperature maximum is attributed to a more subtle interplay between all of these low-lying states.

V. SUMMARY

In this paper, we explored the influence of the NNN coupling $J_2 \leq 0.25|J_1|$ on the thermodynamic properties of the 1D spin-1/2 Heisenberg ferromagnet using ED and RGM methods. The results of both methods are in qualitatively good agreement. We found that the critical behavior of the susceptibility χ and the correlation length ξ is not changed by the frustrating J_2. However, $\lim_{T\to 0} \chi T^2$ and $\lim_{T\to 0} \xi T$ go to zero for $J_2 \to 0.25|J_1|$ indicating a change in the low-temperature behavior of χ (ξ) from $\chi \propto T^{-2}$ ($\xi \propto T^{-1}$) at $J_2 < 0.25|J_1|$ to $\chi \propto T^{-3/2}$ ($\xi \propto T^{-1/2}$) at the critical point $J_2 = 0.25|J_1|$. Another interesting feature is the appearance of a double-maximum structure in the specific heat C_V, where the additional frustration-induced low-temperature maximum was found by ED (RGM) to occur for $J_2/|J_1| \gtrsim 0.125$ (0.16).

ACKNOWLEDGMENTS

This work was supported by the DFG (Projects No. RI615/16-1 and No. DR269/3-1). One of us (S.-L.D.) is indebted to V. Ya. Krivnov for useful discussions. Further discussions with S. Sachdev and A. Zvyagin are kindly acknowledged.

[1] *Quantum Magnetism*, Lecture Notes in Physics Vol. 645, edited by U. Schollwöck, J. Richter, D. J. J. Farnell, and R. F. Bishop (Springer-Verlag, Berlin, 2004).

[2] H.-J. Mikeska and A. K. Kolezhuk, in *Quantum Magnetism*, Lecture Notes in Physics Vol. 645, edited by U. Schollwöck, J. Richter, D. J. J. Farnell, and R. F. Bishop (Springer, Berlin, 2004), p. 1.

[3] T. Tonegawa and I. Harada, J. Phys. Soc. Jpn. **58**, 2902 (1989).

[4] A. V. Chubukov, Phys. Rev. B **44**, 4693 (1991).

[5] F. Heidrich-Meisner, A. Honecker, and T. Vekua, Phys. Rev. B **74**, 020403(R) (2006).

[6] H. T. Lu, Y. J. Wang, Shaojin Qin, and T. Xiang, Phys. Rev. B **74**, 134425 (2006).

[7] D. V. Dmitriev and V. Ya. Krivnov, Phys. Rev. B **73**, 024402 (2006); D. V. Dmitriev, V. Ya. Krivnov, and J. Richter, *ibid.* **75**, 014424 (2007).

[8] R. O. Kuzian and S.-L. Drechsler, Phys. Rev. B **75**, 024401 (2007).

[9] L. Kecke, T. Momoi, and A. Furusaki, Phys. Rev. B **76**, 060407(R) (2007).

[10] D. V. Dmitriev and V. Ya. Krivnov, Phys. Rev. B **77**, 024401 (2008).

[11] R. Zinke, S.-L. Drechsler, and J. Richter, arXiv:0807.3431v1 (unpublished).

[12] B. J. Gibson, R. K. Kremer, A. V. Prokofiev, W. Assmus, and G. J. McIntyre, Physica B **350**, E253 (2004).

[13] T. Masuda, A. Zheludev, A. Bush, M. Markina, and A. Vasiliev, Phys. Rev. Lett. **92**, 177201 (2004).

[14] A. A. Gippius, E. N. Morozova, A. S. Moskvin, A. V. Zalessky, A. A. Bush, M. Baenitz, H. Rosner, and S.-L. Drechsler, Phys.

Rev. B **70**, 020406(R) (2004).
[15] M. Enderle, C. Mukherjee, B. Fak, R. K. Kremer, J.-M. Broto, H. Rosner, S.-L. Drechsler, J. Richter, J. Málek, A. Prokofiev, W. Assmus, S. Pujol, J.-L. Raggazoni, H. Rakato, M. Rheinstädter, and H. M. Ronnow, Europhys. Lett. **70**, 237 (2005).
[16] T. Masuda, A. Zheludev, A. Bush, M. Markina, and A. Vasiliev, Phys. Rev. Lett. **92**, 177201 (2004); S.-L. Drechsler, J. Málek, J. Richter, A. S. Moskvin, A. A. Gippius, and H. Rosner, *ibid.* **94**, 039705 (2005).
[17] S.-L. Drechsler, J. Richter, A. A. Gippius, A. Vasiliev, A. S. Moskvin, J. Málek, Y. Prots, W. Schnelle, and H. Rosner, Europhys. Lett. **73**, 83 (2006).
[18] S.-L. Drechsler, J. Richter, R. Kuzian, J. Málek, N. Tristan, B. Büchner, A. S. Moskvin, A. A. Gippius, A. Vasiliev, O. Volkova, A. Prokofiev, H. Rakato, J.-M. Broto, W. Schnelle, M. Schmitt, A. Ormeci, C. Loison, and H. Rosner, J. Magn. Magn. Mater. **316**, 306 (2007).
[19] S. Park, Y. J. Choi, C. L. Zhang, and S.-W. Cheong, Phys. Rev. Lett. **98**, 057601 (2007).
[20] S.-L. Drechsler, O. Volkova, A. N. Vasiliev, N. Tristan, J. Richter, M. Schmitt, H. Rosner, J. Málek, R. Klingeler, A. A. Zvyagin, and B. Büchner, Phys. Rev. Lett. **98**, 077202 (2007).
[21] J. Málek, S.-L. Drechsler, U. Nitzsche, H. Rosner, and H. Eschrig, Phys. Rev. B **78**, 060508(R) (2008).
[22] H. P. Bader and R. Schilling, Phys. Rev. B **19**, 3556 (1979).
[23] C. P. Landee and R. D. Willett, Phys. Rev. Lett. **43**, 463 (1979); C. Dupas, J. P. Renard, J. Seiden, and A. Cheikh-Rouhou, Phys. Rev. B **25**, 3261 (1982).
[24] M. Takahashi, P. Turek, Y. Nakazawa, M. Tamura, K. Nozawa, D. Shiomi, M. Ishikawa, and M. Kinoshita, Phys. Rev. Lett. **67**, 746 (1991).
[25] J. Kondo and K. Yamaji, Prog. Theor. Phys. **47**, 807 (1972); H. Shimahara and S. Takada, J. Phys. Soc. Jpn. **60**, 2394 (1991); S. Winterfeldt and D. Ihle, Phys. Rev. B **56**, 5535 (1997).
[26] W. Yu and S. Feng, Eur. Phys. J. B **13**, 265 (2000); L. Siurakshina, D. Ihle, and R. Hayn, Phys. Rev. B **64**, 104406 (2001); B. H. Bernhard, B. Canals, and C. Lacroix, *ibid.* **66**, 104424 (2002); D. Schmalfuß, J. Richter, and D. Ihle, *ibid.* **70**, 184412 (2004); I. Juhász Junger, D. Ihle, and J. Richter, *ibid.* **72**, 064454 (2005); D. Schmalfuß, J. Richter, and D. Ihle, *ibid.* **72**, 224405 (2005); D. Schmalfuß, R. Darradi, J. Richter, J. Schulenburg, and D. Ihle, Phys. Rev. Lett. **97**, 157201 (2006).
[27] I. Junger, D. Ihle, J. Richter, and A. Klümper, Phys. Rev. B **70**, 104419 (2004).
[28] T. N. Antsygina, M. I. Poltavskaya, I. I. Poltavsky, and K. A. Chishko, Phys. Rev. B **77**, 024407 (2008).
[29] I. Juhász Junger, D. Ihle, L. Bogacz, and W. Janke, Phys. Rev. B **77**, 174411 (2008).
[30] J. Schulenburg, program package SPINPACK, http://www-e.uni-magdeburg.de/jschulen/spin/
[31] W. Gasser, E. Heiner, and K. Elk, *Greensche Funktionen in Festkörper- und Vielteilchenphysik* (Wiley, Berlin, 2001).
[32] M. Yamada and M. Takahashi, J. Phys. Soc. Jpn. **55**, 2024 (1986).
[33] M. Yamada, J. Phys. Soc. Jpn. **59**, 848 (1990).
[34] P. Kopietz, Phys. Rev. B **40**, 5194 (1989).
[35] F. Suzuki, N. Shibata, and C. Ishi, J. Phys. Soc. Jpn. **63**, 1539 (1994).
[36] V. Ya. Krivnov and D. V. Dmitriev (private communication).
[37] M. Takahashi, Phys. Rev. Lett. **58**, 168 (1987).